

Stem/Leaf Anatomy of Aragoa (Plantaginaceae)

Subjects: [Plant Sciences](#)

Contributor: Alexei Oskolski

Aragoa is a shrubby genus endemic to páramo in the northern Andes representing the sister group to *Plantago* and *Limosella*. Stem and leaf structure of *Aragoa corrugatifolia* were studied to clarify the evolutionary pathways and ecological significance of their anatomical traits. Aragoa and *Plantago* share a non-fascicular primary vascular system, rayless wood and secondary phloem, and anomocytic stomata. Aragoa is distinctive from most Plantaginaceae in the presence of cortical aerenchyma and of helical thickenings in vessels. Its procambium emerges in the primary meristem ring as a continuous cylinder. The view on the ring meristem and procambial strands as developmental stages in the formation of a primary vascular system is not relevant for Aragoa, and probably for other Plantaginaceae. The raylessness is synapomorphic for the crown clade of Plantaginaceae comprising Aragoa, *Littorella*, *Plantago*, *Veronica*, *Picrorhiza*, *Wulfenia*, and *Veronicastrum*. The loss of rays is thought to be predetermined by procambium rather than by the vascular cambium. The extremely narrow vessels with helical thickenings are presumably adaptive to hydric and thermic conditions of páramo. Cortical aerenchyma is thought to be a response to the local hypoxia caused by the water retained by ericoid leaves. Trichomes on juvenile leaves are expected to be the traits of considerable taxonomic importance.

rayless wood

secondary phloem

stomata

trichomes

procambium

aerenchyma

páramo

Plantago

1. Introduction

The rayless wood is a prominent feature of *Aragoa* ^[1]. This uncommon wood trait is also known in the majority of *Plantago* species as well as in some other members of Plantaginaceae ^{[2][3][4][5][6][7][8][9][10]}. The loss of rays can be contingent on different functional, adaptive, and/or morphogenetic factors; particularly, it may be considered as an indicator of secondary woodiness, i.e., the origin of woody habit from herbaceous ancestor ^[5]. Such explanation sounds plausible for mostly herbaceous Plantaginaceae. The evolution of the gains and losses of rays has not been analysed yet for this group and for any other plant family as well.

According to ^{[4][5][11]}, the raylessness in Plantaginaceae can also be considered as a manifestation of wood paedomorphosis, or protracted juvenilism. Following this theory, the rays can be lost due to retaining their absence in juvenile primary xylem at the adult developmental stage, i.e., at the secondary xylem formed by vascular cambium. Moreover, the available data (e.g., ^{[3][6][7][8][12][13][14][15][16][17][18]}) show that the members of Plantaginaceae have a continuous procambium cylinder that gradually goes into the vascular cambium. These

data are in contrast to a common view on the formation of a vascular system, supposing the initiation of procambium as separated strands, giving rise to discrete vascular bundles and the formation of vascular cambium from fascicular and interfascicular cambia at the later stage of shoot development (e.g., [19][20]). At the same time, the procambial ring can contain the ray initials, as it has been reported in many plant groups [21][22][23][24][25] contrarily to a widely held view that the formation of rays is confined to secondary tissues [19]. These data suggest that the presence or absence of ray initials in procambial ring can predetermine their occurrence in vascular cambium and, therefore, it can facilitate the paedomorphic retaining of ray formation or raylessness in secondary tissues. This hypothesis on the role of procambial ring in the formation of rayless wood can be tested by the examination of development of procambium, cambium, and vascular system in a rayless taxon, such as *Aragoa*.

2. Analysis on Research Results

2.1. Development of Meristematic and Conductive Tissues in Stem

Shoot apical meristem (SAM) is about 200 μm in diameter, surrounded with the leaf primordia and small leaves arranged with the $3/8$ phyllotaxis (**Figure 1A,B**). The procambium is initiated in the peripheral zone of SAM (primary meristem) near the shoot tip. The procambial strands are hardly distinguished, forming nearly continuous ring of four to six cells wide, occasionally interrupted by the offsets of leaf traces (**Figure 1A–D**). The procambial cells are angular isodiametric (6–9 μm in width) in transverse view, and elongated (26–48 μm in length) on longitudinal sections. Differentiation of the protoxylem and protophloem begins almost immediately with the formation of groups of one to two helical tracheary elements and one to three sieve elements (**Figure 1E,F**).

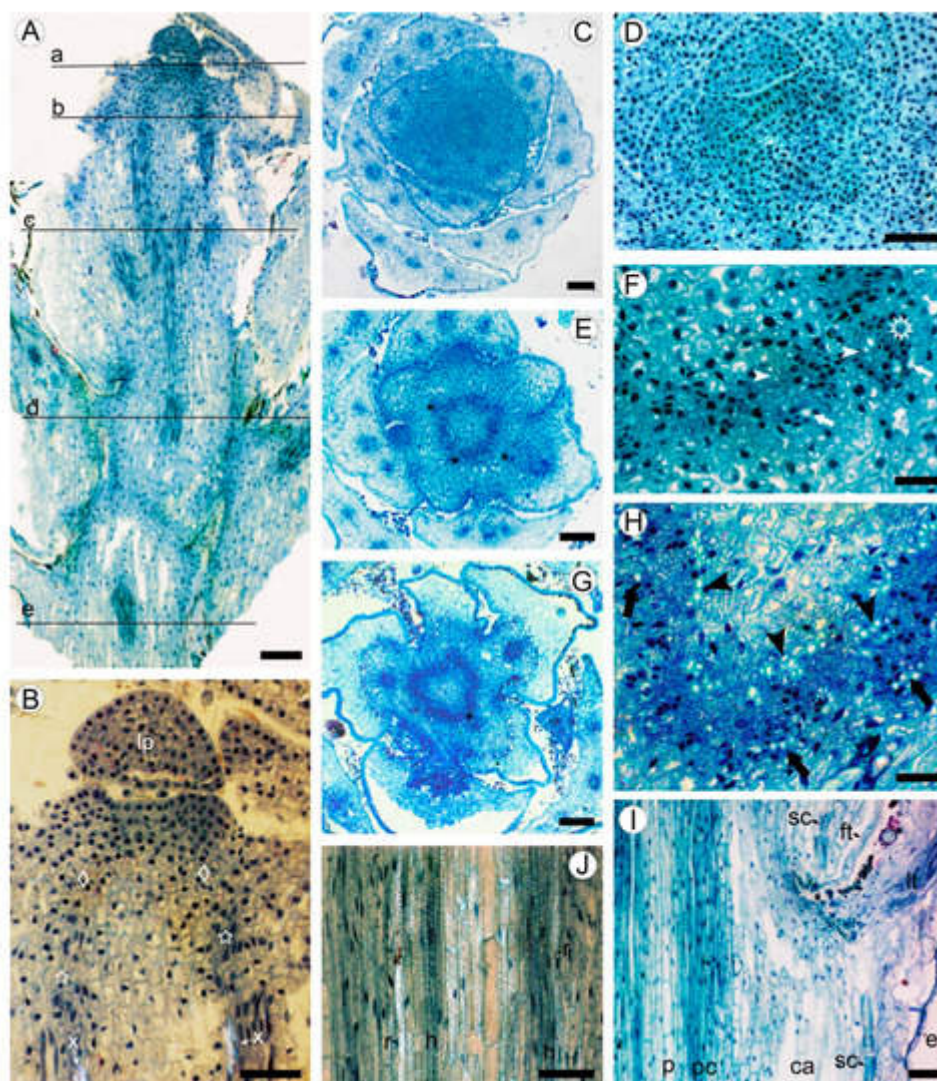


Figure 1. Apical meristem and primary tissues in young shoot of *Aragoa corrugatifolia*, light microscopy (LM). (A) Radial longitudinal section (RLS) of young shoot, approximate positions of the transverse sections (TS) shown on **Figure 1C,D** (a), **Figure 1E,F** (b), **Figure 1G,H** (c), **Figure 1I,J** (d), and **Figure 2A,B** (e); (B) tip of young shoot observed in partially polarized light (RLS), shoot apical meristem (SAM) with leaf primordium (lp) and peripheral zone (diamonds), procambium cells (stars), protoxylem elements (x); (C) shoot tip at the SAM level (TS), 3/8 phyllotaxis, leaf primordia with solitary leaf traces, young leaves with three vascular bundles; (D) SAM with leaf primordia (TS); (E) shoot tip just below the SAM level (TS); procambium ring, leaf traces (asterisks); (F) portion of the procambium ring shown on **Figure 1E** (TS), leaf trace (asterisk), protoxylem (arrowheads), and protophloem (arrows) elements; (G) young shoot in the lower portion of first elongated internode (TS), procambium ring, offset of leaf trace (asterisk). (H) Portion of the procambium ring shown on **Figure 1G** (TS), radial seriations of procambial cells, elements of primary xylem (arrowheads) and primary phloem (arrows); (I) stem and leaf base at the level of fifth elongated internode (RLS), procambium ring (pc), pith (p), cortical aerenchyma (ca), sclereids at the leaf base (sc), epidermis, leaf trace (lt), filiform trichome (ft); (J) portion of the procambium ring shown in **Figure 1I** observed in partially polarized light (RLS), tracheary elements with helical (h) and reticulate (r) patterns of secondary cell wall. Scale bars: 100 μm for (A,C,E,G), 50 μm for (B,D,I,J), 20 μm for (F,H).

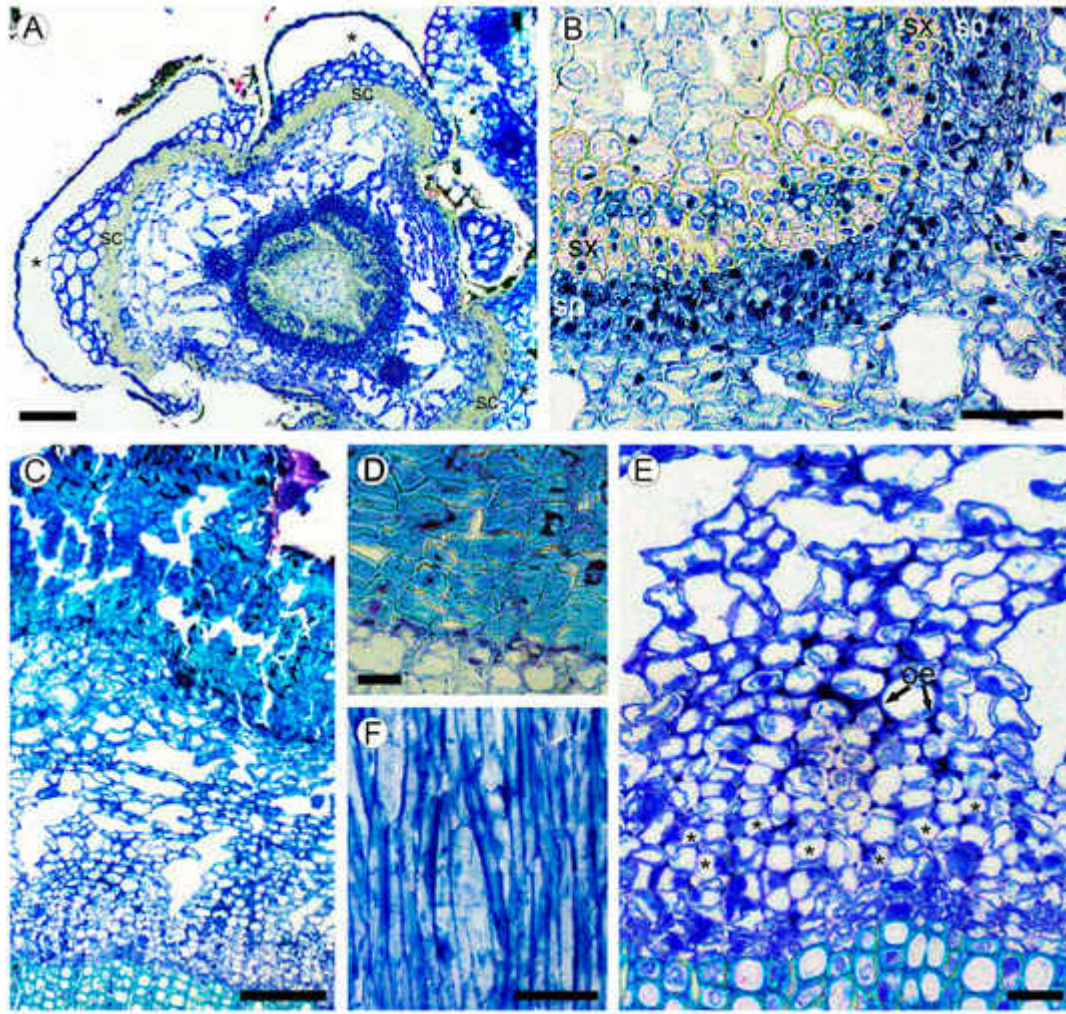


Figure 2. (A,B) Structure of young stem in *Aragoa corrugatifolia* (LM). (A) Young shoot with prominent leaf bases in the lower portion of fourth elongated internode (TS), vascular cambium with juvenile rings of secondary xylem and secondary phloem, cortical aerenchyma, leaf bases (asterisks) outlined with the bands of sclereids (sc); (B) portion of the ring of secondary conductive tissues shown in **Figure 2A** (TS), continuous rings of secondary xylem (sx) and secondary phloem (sp). (C–F) Structure of mature bark. (C) Secondary phloem, cortex with aerenchyma, periderm with uniseriate phelloderm, and prominent phellem made of thick-walled cell (TS); (D) Portion of periderm, phellem cells with thick sclerified walls, thin-walled phelloderm cells in one to two layers (TS); (E) portion of secondary phloem and cortical aerenchyma shown in **Figure 2C** (TS), sieve tubes with companion cells in radial groups (*), obliterated phloem elements (oe), large intercellular spaces in cortex; (F) tangential longitudinal section (TLS) of secondary phloem; strands of phloem axial parenchyma, lack of rays. Scale bars: 100 μm for (A,C), 50 μm for (B,F), 20 μm for (D,E).

At the level of the base of the first elongated internode (ca. 0.4 mm from the apex), the procambium ring widens up to 7–10 cells wide, interrupted only by the gaps at the offsets of leaf traces (**Figure 1G,H**). The procambial cells in the ring show a tendency for radial seriation; the sites of leaf trace initiation can be distinguished as the clusters of cells divided at various orientations. The elements of primary phloem are in groups of two to four scattered along the outer side of the procambium ring. These tracheary elements are solitary and grouped as two to five cells,

found in the inner region of procambium ring, without obvious association with the groups of phloem elements. The proto- and metaxylem consists of tracheary elements with helical and reticulate patterns of secondary cell walls.

In the lower internodes, the vertical length of procambium cells increases due to the shoot growth up to 35–67 μm in the fifth internode (**Figure 1I,J**). These cells are more tapered than those near the shoot tip. Some cells undergo transverse divisions, forming the strands of two cells. No short procambium cells resembling the ray initials were found. Below the sixth internode, the procambium ring is gradually transformed into the vascular cambium, which is recognized by the appearance of the continuous rings of regularly arranged phloem and xylem elements around the pith made of thin-walled isodiametric parenchyma cells of 15–25 μm , with large intercellular spaces in between. Sclereids with moderately thick cell walls were found in the outermost region of pith (**Figure 2A,B**).

2.2. Bark Structure

A large portion of the circumference of young stems is occupied by the bases of leaves covered with the leaf abaxial epidermis. The zones of attachment of leaf bases to the stem cortex are outlined with the uniseriate (occasionally biseriate) layers of thick-walled vertically elongated sclereids of 18–34 μm in tangential size and 32–54 μm in vertical size (**Figure 1J** and **Figure 2A**). Between the leaf bases, the epidermis on young parts of stems is composed of a single layer of isodiametric cells (15–25 μm in tangential size) with evenly thick walls (3–7 μm thick) covered by a prominent cuticle that is 8–10 μm thick, with dark deposits. The cortex is narrow (10–12 cells in width) and composed of aerenchyma made isodiametric to elongated thin-walled parenchyma cells of 15–35 μm in size, with large intercellular spaces in-between. No crystals were found in the cortical parenchyma cells. Primary phloem fibers were absent (**Figure 2A,B**). Dilation of the cortical tissue is effected mostly by tangential stretching of parenchyma cells and intercellular spaces.

Mature bark is dark brown, non-peeling, without fissures and scales. The initiation of periderm is in the subepidermal layer of cells. The phellem is composed of 8–15 layers isodiametric to somewhat flattened cells with thick to very-thick sclerified cell wall occasionally with dark deposits. The phelloderm comprises one to two layers of isodiametric, thin-walled cells. No crystalliferous cells were found in periderm. Subsequent periderms were not found (**Figure 2C,D**).

Sieve tubes are in radial groups of two to seven. Sieve tubes members are 148–236 μm (average 184.2 μm) in length and are 9–18 μm wide. Sieve plates are compounded with two to three sieve areas, located on vertical or slightly oblique cross walls. Axial parenchyma cells are associated with conducting elements that occur as single fusiform cells and in strands of two to three cells. The transition from conducting to nonconducting secondary phloem is gradual, marked with obliterated conductive cells and slightly tangentially stretched axial parenchyma cells (**Figure 2E**). Secondary phloem rays were not found (**Figure 2F**).

2.3. Leaf Structure

Leaves are linear, 1–2 mm in width, sessile, with convex abaxial side, and flat adaxial surface, and are 200–400 μm thick. The adaxial epidermal cells do not differ from the abaxial ones in their shape and size; these cells are

flattened to isodiametric, 18–30 μm in tangential size, with even walls of approximately 1 μm thick (**Figure 3A,B**). Hydathode pores are present at the leaf tips (**Figure 3C**).

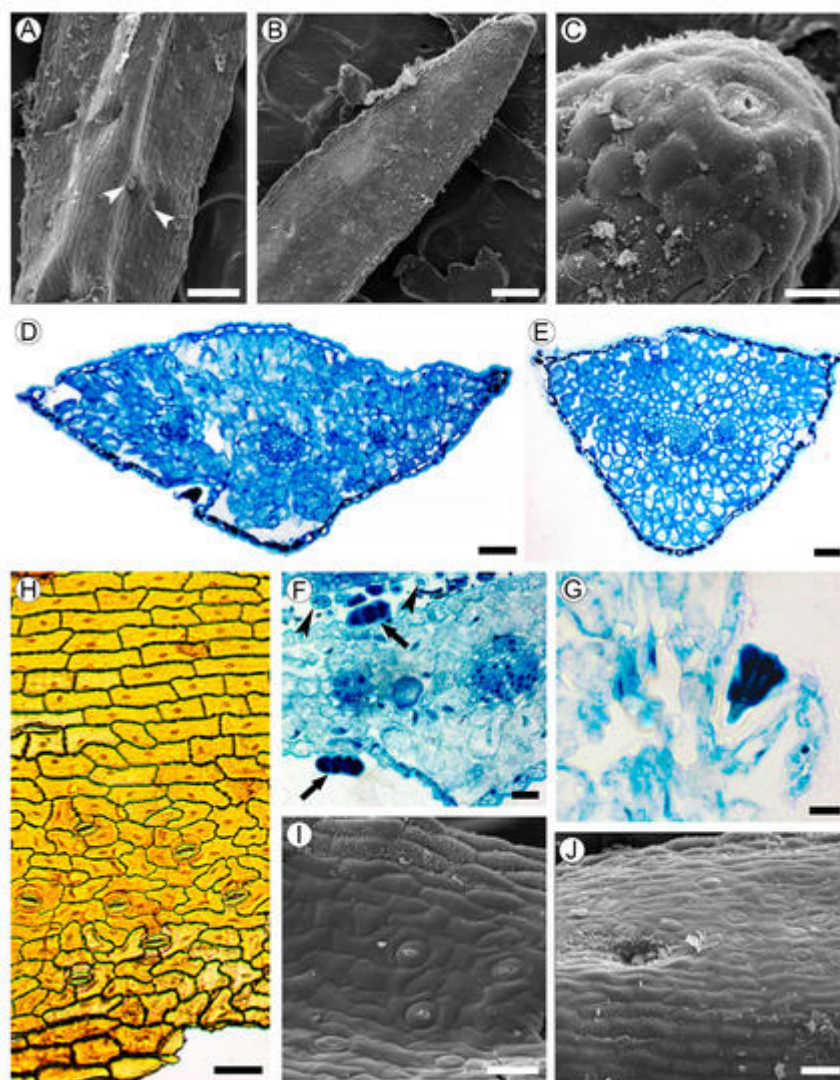


Figure 3. Leaf structure of *Aragoa corrugatifolia*. (**A**) Abaxial leaf side (SEM), sessile glandular trichomes (arrowheads); (**B**) adaxial leaf side (SEM), hydathode pore on the leaf tip; (**C**) hydathode pore at the leaf tip shown on **Figure 3B** (SEM); (**D**) TS of leaf in its middle portion (LM), epidermis with prominent cuticle, spongy mesophyll, three vascular bundles; (**E**) TS of leaf in its basal portion (LM), epidermis with prominent cuticle, spongy mesophyll, branch point of vascular bundles; (**F**) fragment of leaf (TS, LM), sessile glandular trichomes on adaxial and abaxial epidermis (arrows), cross sections of filiform trichomes (arrowheads); (**G**) stalked glandular trichome on adaxial epidermis (LM); (**H**) Abaxial epidermis (LM) from midrib without stomata (top) and lateral portions of leaf with anomocytic stomata (bottom). (**I**) Adaxial leaf side (SEM), anomocytic stomata, epidermal cells with curved anticlinal walls. (**J**) Midrib region on adaxial leaf side (SEM), epidermal cells with straight anticlinal walls, hollow with glandular trichome. Scale bars: 200 μm for (**A,B**), 50 μm for (**C–E,H–J**), 20 μm for (**F,G**).

Leaf blades are isobilateral (**Figure 3D,E**). The spongy mesophyll consists of irregularly shaped cells of 11–25 μm in size with large intercellular spaces. The vascular bundles are collateral, sheathed by one or two layers of

parenchyma cells without lateral or vertical extensions. Each leaf is supplied by a single trace that is forked into three vascular bundles near the leaf base.

Long (3–4 mm in length) multicellular filiform trichomes are found at the bases of juvenile leaves on their adaxial sides, and usually lack mature leaves (**Figure 1I** and **Figure 3F**). Glandular trichomes sessile or on unicellular stalks, with four head cells, are located mostly in hollows sparsely scattered on both leaf sides (**Figure 3A,F,G,J**).

Anticlinal walls of epidermal cells are mostly straight in the midrib region, or mostly curved outside of it. The outer walls of the epidermal cells are covered by a cuticle of approximately 4–7 μm thick. Leaves are amphistomatic; stomata are more numerous on the abaxial side (48–62 per mm^2) than on the adaxial side (39–50 per mm^2), lacking in the midrib region. Stomata anomocytic is located in the same plane with epidermal cells (**Figure 3H–J**).

2.4. Wood Structure

Growth rings absent. Wood is rayless (**Figure 4A–C**). Vessels are angular; rarely rounded in outline; extremely narrow with a tangential diameter of 9.2–19 μm (average 13.5 μm); and are extremely numerous (1130–1700 per mm^2), mostly solitary, and also has multiples. Vessel walls are 1.6–3.4 μm thick. Tyloses were not found. Vessel elements are 102–275 μm long (average 202.6 μm). Perforation plates are simple. Intervessel pits are alternate and minute, 1.8–3.5 μm in vertical size, mostly with rounded margins and slit-like apertures. Helical thickenings throughout the body of the vessel element are common (**Figure 4D–F**). Ground tissue elements are non-septate libriform fibers of 190–317 μm (average 255.2 μm) in length, mostly with living protoplast and nuclei. Fiber walls are 2.0–5.4 μm thick, with distinctly bordered pits of 2.4–3.5 μm in vertical size, with slit-like apertures in radial and tangential walls. Axial parenchyma was not observed.

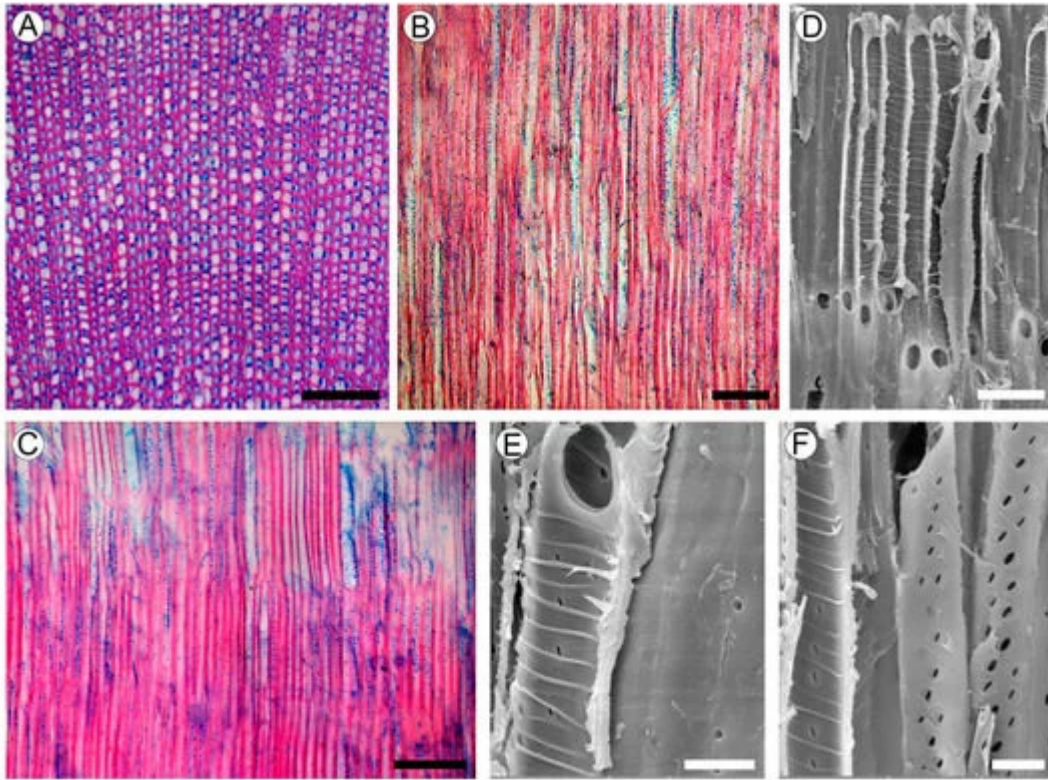


Figure 4. Wood structure of *Aragoa corrugatifolia*. (A) TS of wood (LM), growth rings absent, very narrow vessels, libriform fibers with living protoplasts; axial parenchyma and rays absent; (B) TLS of wood (LM), very narrow vessels, lack of rays; (C) RLS of wood (LM), imperforate elements with numerous pits in radial walls, lack of rays; (D) vessel elements on RLS (SEM), simple perforation plates, helical thickenings on vessel walls; (E) vessel element and fibriform fiber on RLS (SEM), simple perforation plates, helical thickenings on vessel walls, pits on the fiber wall (right); (F) vessel elements on RLS (SEM), helical thickenings on vessel walls; minute intervessel pits. Scale bars: 100 µm for (A–C), 10 µm for (D–F).

2.5. Evolution of Rayless Wood within Plantaginaceae

Both our observations on *Aragoa*, and the published wood anatomical data on other Plantaginaceae genera [26][2][3][4][6][7][8][9][10][16][18][27][28], were used to reconstruct the pattern of evolution for the raylessness within this family (Figure 5). The mapping of this trait on a subset of the most parsimonious tree of the combined analysis of one nuclear and three plastid regions [29] shows that the loss of rays is synapomorphic for the large crown clade comprising the genera *Aragoa*, *Littorella*, *Plantago*, *Veronica*, *Picrorhiza*, *Wulfenia*, and *Veronicastrum*, and it occurred twice independently in the genera *Erinus* and *Digitalis*, belonging to its sister lineage.

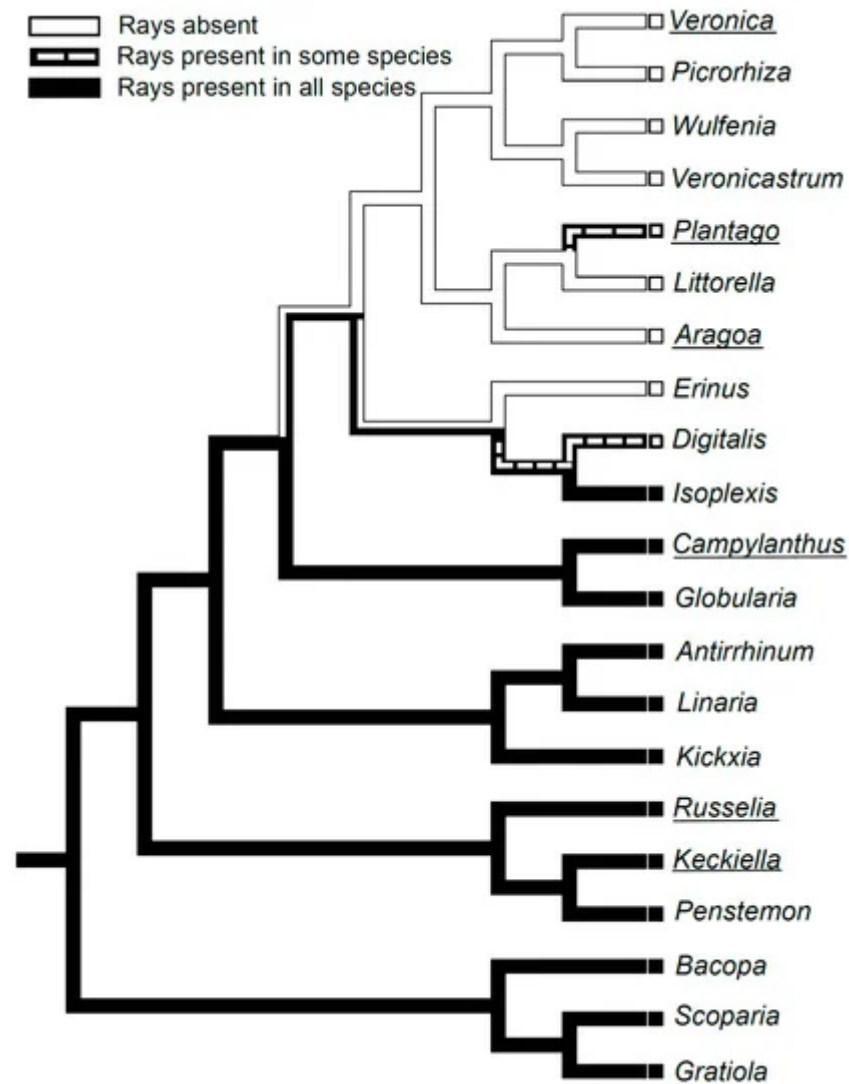


Figure 5. Distribution of the presence or absence of rays in the wood mapped onto a subsample of the most parsimonious tree of the combined analysis of one nuclear and three plastid regions for the family Plantaginaceae [30]. The genus *Littorella* was added to this tree following [31]. The names of genera containing shrubby species are underlined; other genera are herbaceous.

References

1. Mennega, A.M.W. On unusual wood structures in Scrophulariaceae. *Acta Bot. Neerl.* 1975, 24, 359–360.
2. Dill, F.E. Morphology of *Veronicastrum virginicum*. *Trans. Kansas Acad. Sci.* 1941, 44, 158–163.
3. Metcalfe, C.R.; Chalk, L. *Anatomy of the Dicotyledons*; Clarendon Press: Oxford, UK, 1950; Volume 2, pp. 1052–1059.
4. Carlquist, S. Wood anatomy of insular species of *Plantago* and the problem of raylessness. *Bull. Torrey Bot. Club* 1970, 97, 353–361.

5. Carlquist, S. Living cells in wood. 2. Raylessness: Histology and evolutionary significance. *Bot. J. Linn. Soc.* 2015, 178, 529–555.
6. Schweingruber, F.H.; Börner, A.; Schulze, E.-D. Atlas of Stem Anatomy in Herbs, Shrubs und Trees; Springer: Berlin/Heidelberg, Germany, 2011; Volume 2, pp. 1–415.
7. Schweingruber, F.; Landolt, W. The Xylem Database. Swiss Federal Institute for Forest, Snow and Landscape Research. 2010. Available online: <https://www.wsl.ch/dendropro/xylemdb/> (accessed on 10 April 2021).
8. Kaplan, A.; Hasanoğlu, A.; Ikbal, A.I. Morphological, anatomical and palynological properties of some Turkish Veronica L. species (Scrophulariaceae). *Int. J. Bot.* 2007, 3, 23–32.
9. Ida Christi, V.E.; Senthamarai, R. Qualitative and quantitative pharmacognostical studies on *Scoparia dulcis* Linn leaf. *Int. J. Pharm. Pharmaceut. Res.* 2015, 3, 57–74.
10. Doležal, J.; Dvorský, M.; Börner, A.; Wild, J.; Schweingruber, F.H. Anatomy, Age and Ecology of High Mountain Plants in Ladakh, the Western Himalaya; Springer: Cham, Switzerland, 2018; p. 616.
11. Carlquist, S. A theory of pedomorphosis in dicotyledonous woods. *Phytomorphology* 1962, 12, 30–45.
12. Kostytschew, S. Der Bau und das Dickenwachstum der Dikotylenstämme. *Ber. Dtsch. Bot. Ges.* 1922, 40, 297–305.
13. Kostytschew, S. Der Bau und das Dickenwachstum der Dikotylenstämme. *Beih. Bot. Zentralbl.* 1924, 40, 295–350.
14. Helm, J. Untersuchungen über die Differenzierung der Sprossscheitelmeristeme von Dikotylen, unter besonderer Berücksichtigung des Prokambiums. *Planta* 1931, 15, 105–191.
15. Krumbiegel, A.; Kästner, A. Sekundäres Dickenwachstum von Sproß und Wurzel bei annuellen Dicotylen. *Biosyst. Ecol.* 1993, 4, 1–49.
16. Hussain, K. *Bacopa monnieri* (L.) Lennell—A good biomarker of water pollution/contamination. *J. Stress Physiol. Biochem.* 2010, 6, 91–101.
17. Hamed, K.A.; Hassan, S.A.; Mohamed, A.-S.H.; Hosney, N.K. Morphological and anatomical study on Plantaginaceae Juss. and some related taxa of Scrophulariaceae Juss. *Egypt. J. Exp. Biol. Bot.* 2014, 10, 135–146.
18. Ahmed, E.M.; Desoukey, S.Y.; Fouad, M.A.; Kamel, M.S. A pharmacognostical study of *Russelia equisetiformis* Sch. & Cham. *Int. J. Pharmacog. Phytochem. Res.* 2016, 8, 174–192.
19. Beck, C.B. An Introduction to Plant Structure and Development; Plant Anatomy for the Twenty-First Century; Cambridge University Press: Cambridge, CA, USA, 2010; pp. 1–464.

20. Claßen-Bockhoff, R.; Franke, D.; Krämer, H. Early ontogeny defines the diversification of primary vascular bundle systems in angiosperms. *Bot. J. Linn. Soc.* 2021, 195, 281–307.
21. Cumbie, B.G. Development and structure of the xylem in *Canavalia* (Leguminosae). *Bull. Torrey Bot. Club* 1967, 94, 162–175.
22. Cumbie, B.G. Developmental changes in the xylem and vascular cambium of *Apocynum sibiricum*. *Bull. Torrey Bot. Club* 1969, 96, 629–640.
23. Soh, W.Y. Early ontogeny of vascular cambium II. *Aucuba japonica* and *Weigela coraeensis*. *Bot. Mag.* 1974, 87, 17–32.
24. Soh, W.Y. Early ontogeny of vascular cambium III. *Robinia pseudo-acacia* and *Syringa oblata*. *Bot. Mag.* 1974, 87, 99–112.
25. Myśkow, E. Procambium–cambium transition during vascular meristem development in *Diospyros lotus*. *Botany* 2010, 88, 985–993.
26. InsideWood. 2004-Onwards. Available online: <http://insidewood.lib.ncsu.edu/> (accessed on 10 April 2021).
27. Michener, D.S. Wood and leaf anatomy of *Keckiella* (Scrophulariaceae): Ecological considerations. *Aliso* 1981, 10, 39–57.
28. Kalashnikova, O.A.; Bildanova, L.I.; Ryzhov, V.M.; Tarasenko, L.V. Morphological and anatomical analysis of *Gratiola officinalis* L. In *Pharmaceutical Botany: Its Present State and Perspectives*; Kurkin, V.A., Ed.; SamGMU: Samara, Russia, 2017; pp. 92–103. (In Russian)
29. Albach, D.C.; Meudt, H.M.; Oxelman, B. Piecing together the “new” Plantaginaceae. *Am. J. Bot.* 2005, 92, 297–315.
30. Mower, J.P.; Guo, W.; Partha, R.; Fan, W.; Levsen, N.; Wolff, K.; Nugent, J.M.; Pabón-Mora, N.; González, F. Plastomes from tribe Plantagineae (Plantaginaceae) reveal infrageneric structural synapomorphies and localized hypermutation for *Plantago* and functional loss of *ndh* genes from *Littorella*. *Mol. Phylogenet. Evol.* 2021, 162, 107217.
31. Hoggard, R.K.; Kores, P.J.; Molvray, M.; Hoggard, G.D.; Broughton, D.A. Molecular systematics and biogeography of the amphibious genus *Littorella* (Plantaginaceae). *Am. J. Bot.* 2003, 90, 429–435.

Retrieved from <https://encyclopedia.pub/entry/history/show/32511>